Contrib Mineral Petrol (1995) 121:388–399

Thomas J. Williams · Philip A. Candela · Philip M. Piccoli

The partitioning of copper between silicate melts and two-phase aqueous fluids: An experimental investigation at 1 kbar, 800° C and 0.5 kbar, 850° C

Received: 27 June 1994/Accepted: 30 March 1995

Abstract Experiments were performed in the three phase system high-silica rhyolite melt + low-salinity aqueous vapor + hydrosaline brine, to investigate the partitioning equilibria for copper in magmatic-hydrothermal systems at 800° C and 1 kbar, and 850° C and 0.5 kbar. $D_{Cu}^{aqm/mlt}$ and apparent equilibrium constants, $K_{Cu,Na}^{aqm/mlt}$, between the aqueous mixture (aqm = quenched vapor + brine) and the silicate melt (mlt) are calculated. $D_{Cu}^{aqm/mlt}$ increases with increasing aqueous chloride concentration and is a function of pressure. $K_{Cu,Na}^{aqm/mlt} = 215(\pm 73)$ at 1 kbar and 800° C and $K_{Cu,Na}^{aqm/mlt} = 11(\pm 6)$ at 0.5 kbar and 850°C. Decreasing pressure from 1 to 0.5 kbar lowers $K_{Cu,Na}^{aqm/mlt}$ by a factor of approximately 20. Data revealed no difference in $K_{Cu,Na}^{aqm/mlt}$ or $D_{Cu}^{aqm/mlt}$ as a function of the melt aluminium saturation index. Within the 2-phase field the $K_{Cu,Na}^{aqm/mlt}$ show no variation with total aqueous chloride, indicating that copper-sodium exchange between the vapor, brine and silicate melt is independent of the mass proportion of vapor and brine. Model copper-sodium apparent equilibrium constants for the hydrosaline brine and the silicate melt revealed a negative dependence on pressure. Model apparent equilibrium constants for copper-sodium exchange between the brine and vapor were close to unity at 1 kbar and 800° C.

Introduction

A fundamental tenet of the magmatic-hydrothermal theory for the formation of porphyry copper deposits involves the separation of magmatic volatile phases from silicate melts, and the preferential segregation of ore metals into that aqueous fluid (Holland 1972; Whitney 1975; Burnham 1967, 1979; Candela and Holland 1984; Dilles 1987; Hedenquist and Lowenstern 1994). To build a better understanding of the formation of porphyry deposits, it is necessary to develop an understanding of ore metal partitioning between melt and aqueous fluids. The propensity of ore metals, such as copper, to partition into the magmatic aqueous phase has been the subject of a number of experimental, theoretical, and field investigations (Ryabchikov et al. 1981; Candela and Holland 1984; Candela 1989a; Keppler and Wyllie 1991; Cline and Bodnar 1991; Lowenstern et al. 1991). Candela and Holland (1984) systematically investigated the partitioning of copper between a silicate melt and the magmatic aqueous phase. Their experiments were conducted at 1.4 kbar and 750° C with a high-silica rhyolite and a NaCl- plus KCl- plus HCl-bearing aqueous phase. Copper partitioning was studied as a function of the chlorine concentration of the aqueous phase. Their data indicate that the aqueous phase/melt partition coefficient for copper is a linear function of the chloride concentration of the aqueous phase. The results of Keppler and Wyllie (1991) indicate a similar proportional relationship at 750° C and 2 kbars in the system haplogranite–H_2O–HCl.

Detailed studies of existing porphyry copper deposits suggest that many are associated with shallow (approximately 1–3 km depth), subvolcanic magmatic systems (Gustafson and Hunt 1975; Titley and Beane 1981). At lithospheric pressures prevailing at these depths, a miscibility gap exists in H_2O-chloride systems consisting of a low salinity aqueous vapor and a hydrosaline liquid or brine (Sourirajan and Kennedy 1962; Bodnar et al. 1985). The presence of coexisting vapor and brine associated with porphyry systems has been confirmed by fluid inclusion studies (Roedder 1979; Bodnar and Beane 1980). Therefore, ore metal partitioning in many, if not most, porphyry copper systems occurs among

T.J. Williams (✉) · P.A. Candela · P.M. Piccoli
Laboratory for Mineral Deposits Research, Department of Geology, University of Maryland at College Park, College Park, MD 20742–4211, USA

Editorial responsibility: T. L. Grove

three phases (vapor + brine + melt). To construct realistic models of porphyry copper systems, it is necessary to gather partitioning data under conditions that lie within the two-phase vapor plus brine field. The purpose of this investigation was to extend the partitioning data for copper to lower pressures and to investigate the effect of subcritical behavior on the partitioning of ore metals in magmatic-hydrothermal systems.

Experiments were conducted at 1 kbar and 800° C, and 0.5 kbar and 850° C. Oxygen fugacity was fixed by the experimental apparatus at approximately two log units above the Nickel-Nickel Oxide (NNO) buffer curve. Naturally occurring Bishop Tuff high-silica rhyolite was selected as the glass starting material. The starting aqueous solutions were mixtures of KCl plus NaCl plus HCl with copper added as $CuCl_2$. Copper partitioning was studied as a function of total chlorine in the aqueous fluids. Experiments were conducted near, but just outside, the low-salinity boundary of the two phase field, and then extended into the two-phase field with increasing total chlorine.

Experiments performed within the two-phase vapor plus brine field were quenched to room temperature and pressure, where the immiscible phases remixed to form a single phase fluid or aqueous mixture. The low salinity aqueous vapor and hydrosaline brine were not analyzed directly.

Data are presented as partition coefficients between the aqueous mixture and the rhyolite melt, and as apparent equilibrium constants for elemental exchange between the bulk mixture and melt. A series of simple algorithms was derived and combined with phase equilibrium data from the system $NaCl–H_2O$, and the data from this study, to model the concentrations of copper and sodium in the aqueous vapor and the hydrosaline brine. By using the modeled concentrations, a series of apparent equilibrium constants is calculated for copper-sodium exchange between the brine, the aqueous vapor, and the silicate melt.

From these apparent equilibrium constants we draw tentative conclusions about the behavior of copper in the system aqueous vapor plus hydrosaline brine plus silicate melt under magmatic-hydrothermal conditions.

Experimental techniques

Starting material

A naturally occurring high-silica rhyolite and prepared solutions of NaCl, KCl, HCl and $CuCl_2$ were employed as starting materials. Fluid/solid ratios were 2:1 for all experiments.

The glass starting material was a Bishop Tuff high-silica rhyolite (pumice fragments) collected from Long Valley California. The Bishop Tuff was selected because it is well characterized, and has a well constrained composition. Hildreth (1979) reported that the Bishop Tuff is a high-silica rhyolite with silica content ranging from 77 wt% to approximately 75 wt%. Table 1 displays analyses of the pumice used as the starting glass in this investigation. The sample's composition does not vary appreciably from the values given by Hildreth (1979).

A high-silica rhyolite was selected as a starting material for practical experimental and analytical reasons. The solidus and liquidus temperatures are low and well constrained. The pumice material was prepared by first grinding it in an agate mortar and pestle and then hand-picking for impurities under a binocular microscope. In addition, large opaque grains were removed with a small magnet.

Starting solutions were prepared by using commercial laboratory reagents of NaCl, KCl, and HCl. Copper was added as anhydrous reagent grade $CuCl_2$. The HCl/ΣCl ratios of the starting solutions ranged from 0.3 to 0.03, and the proportion of $CuCl_2$/ΣCl in all experiments was held constant at approximately 0.06.

HCl/ΣCl in the starting solutions was varied in an attempt to change the melt aluminosity. High HCL/ΣCl should produce silicate glass run products that are more peraluminous versus run products equilibrated with low HCl/ΣCl starting solutions. In the following discussion aluminosity is related as the Aluminium Saturation Index (ASI).

Experimental procedures

Experiments were performed in rapid-quench cold-seal vessels (Cancela and Holland 1984). The vessels were pressurized with water and argon, and heated in solid tube furnaces. The exterior portions of the cold end of the pressure vessel were cooled by a water circulating jacket during the experimental run. At the end of an experimental run the vessel was removed from the furnace and tilted vertically allowing the charge to slide to the cool end of the vessel; the charge

Table 1 Starting melt compositions (Bishop Tuff Rhyolite Glass) recalculated to an anhydrous basis (wt%). 1-sigma uncertainty for the electron probe analyses are listed. Summary of experimental conditions, and the make-up of experimental charges

	Microprobe	XRF[a]	ICP[a]
SiO_2	76.4(± 1.5)	76.4	76.6
TiO_2	0.04(± 0.2)	0.07	0.08
Al_2O_3	14.0(± 0.4)	13.3	13.1
FeO	0.52(+ 0.03)	0.88	0.88
MgO	0.10(± 0.01)	0.12	0.10
CaO	0.46(± 0.1)	0.46	0.49
MnO	0.00(± 0.02)	0.03	0.03
Na_2O	2.83(± 0.13)	2.95	2.93
K_2O	5.67(± 0.3)	5.66	5.75
P_2O_5	n.d.	0.02	0.02
Total	100.02	99.98	99.98

[a]Analysis by Activation Laboratorie Ltd., Ancaster, Ontario, Canada

Experimental conditions
1 kilobar and 800°C
0.5 kilobar and 850°C
Starting solutions
(NaCl + KCl + HCl + $CuCl_2$)
HCl/ΣCl: 0.03 − 0.30
Volumes: 150 ml (1 kbar/800° C)
110 ml (0.5 kbar/850° C)
Bishop Tuff Rhyolite
Mass of starting material:
75 mg (1 kbar/800° C)
55 mg (0.5 kbar/850° C)

was quenched to room temperature in a matter of seconds. Sample temperature was measured with single external Chromel-Alumel thermocouple. Pressure was monitored by using a bourdon tube gauge checked against a factory calibrated Heise gauge.

Temperature gradients were minimized by running the vessels sub-horizontally with the sample-end tilted up 10° as suggested by Charles and Vidale (1982). In this orientation, the temperature gradient within the vessel is less than 5° C over the length of the charge (Candela 1982).

Ground high-silica rhyolite samples (55 or 75 mg) were placed in a platinum capsule. The chloride-bearing aqueous solution was added by micropipette. Table 1 summarizes the masses, volumes, and phase proportions of starting material used in this investigation. The capsule was then crimped, weighed, and sealed with a carbon arc-welder. To minimize volatile loss, the capsule was welded in a metal-foil boat filled with crushed dry ice. The capsule was weighed again after welding to check for volatile loss.

After quenching, the capsule was removed from the pressure vessel, cleaned, and dried. The capsule was weighed to check for significant leakage during the run, and then pierced with a stainless steel hypodermic needle and the solution removed with a sterile plastic syringe. The volume of solution recovered varied from approximately 140 μl (microliters) down to approximately 40 μl. After removal, the solution was diluted with double-distilled deionized water to a volume of 10 ml in a volumetric flask. After the solution was removed, the capsule was split open and the glass removed, rinsed with distilled water, dried, and mounted in a polymer casting resin and polished for microprobe analysis.

In this investigation, the nickel alloy composition of the pressure vessel (René 41) and the pressure medium, water, impose a fixed hydrogen fugacity f_{H_2} at a given temperature and pressure.

The f_{H_2} was measured by using the hydrogen sensor technique developed by Chou (1978), and the f_{O_2} was calculated by using the method described by Chou (1987). Log f_{O_2} values measured in the experimental vessels under run conditions were approximately two log units above the Nickel-Nickel Oxide buffer curve. f_{O_2} was not monitored during individual experimental runs.

Analytical techniques

Determination of cation concentrations in aqueous mixtures

Analyses of the aqueous mixtures were performed by atomic absorption spectrophotometry with an air-acetylene flame to determine the concentration of Na, K, Cu, and Fe. Concentrations were determined by the method of standard addition. Concentrations are listed as parts per million by weight (ppm) and as mols/kg of solution. Internal standards were run as unknowns on a routine basis to check precision and accuracy. Long-term analytical precision for aqueous Na, K, Cu and Fe was approximately 10% (relative).

The total chlorine concentration (ΣCl) of the aqueous solutions was determined by using a time-based titration chloridometer (Labconco Model 442-5100). The technique is based on the coulometric titration of silver ions. Instrument standardization was performed by using a 0.10 mols/kg of a NaCl standard. Analytical precision was approximately ± 4% (relative) as measured by replicate analysis of the NaCl standard solution. Sulfur concentrations in the silicate glass and aqueous mixture were not measured. Sulfur concentration in the starting Bishop tuff pumice was low and we do not believe that its effect is significant.

Electron probe microanalyses of silicate glass

The analyses of the high-silica rhyolite glass were performed on a JEOL JXA 840A electron probe microanalyzer with a Tracor Northern 5500 operating system. Analyses were conducted by quantitative wavelength dispersive spectrometry with the following crystals: TAP (Si, Al, Mg, Na), LiF (Fe, Cu), PET (Ca, K, Cl). Elemental concentrations in the quenched glasses are listed as oxide wt% and element ppm.

The analytical program was accomplished in two steps. First, glasses were analyzed for major elements and chlorine by using an accelerating voltage of 15 kV and a 2.5 nA cup current with a 10 μm by 10 μm rastered beam. Si, Al, K, Na, Fe, and Mg were counted for 30 s with a Yellowstone rhyolite glass standard (Si, Al, Fe, Ca, K), a Kakanui hornblende standard (Mg), and a jadeite standard (Na). A 60 s count-time was employed for chlorine analyses with a Durango apatite and scapolite as standards.

The glasses were reanalyzed separately for the copper at 30 kV and 250 nA by using a 10 μm by 10 μm rastered beam. Analysis time for copper was 180 s with a NIST glass standard (NBS SRM 610) containing approximately 444 ppm Cu. The higher sample current and longer count time was necessary because of the low copper concentrations in the run products. A separate analytical schedule for copper was employed to minimize damage to the silicate glasses until analyses for more volatile elements such as Na and Cl were completed.

Electron probe analytical uncertainties for major and minor elements (at 1-sigma) are listed in Table 1. Analytical uncertainty for chlorine was approximately 2% (relative). Copper was observed at trace concentrations (tens to hundreds of ppm) in the glass run products. Absolute analytical uncertainty for copper in the silicate glass was ± 12 ppm at 1 kbar and ± 85 ppm at 0.5 kbar.

Sodium migration is a common problem of electron microprobe analysis of hydrated silicate glass (Nielsen and Sigurdsson 1981). To compensate for this problem, sodium was placed first in the analytical schedule, and determined by using a low sample current, a wide beam diameter, and a short counting time (30 s). The low power beam and short counting time increased overall analytical uncertainty but allowed for the collection of more accurate sodium data.

In an attempt to determine the extent of sodium migration under these analytical conditions, a series of sodium analyses were conducted on the same sample point. Inspection of sodium counts/s/nA versus time indicated that, under the above analytical conditions for the major elements, sodium loss was within the analytical uncertainty for an analysis of 30 s duration.

Immiscibility in the magmatic aqueous phase

The importance of vapor-brine immiscibility to hydrothermal ore formation has been recognized by numerous investigators (Bodnar and Beane 1980; Burnham and Ohmoto 1980; Roedder 1984; Brimhall and Crerar 1987; Dilles 1987). However, the effect of immiscibility on the chemistry of hydrothermal fluids and silicate melts has gone largely unstudied. Exceptions are experimental studies by Shinohara (1987) and Shinohara et al. (1989) and theoretical discussions by Candela (1989a) and Cline and Bodnar (1991).

Under the conditions of this study (800° C to 850° C and 1 to 0.5 kbar total pressure), the starting aqueous fluids lie within an immiscible two-phase field where a low-salinity aqueous vapor coexists with a hydrosaline liquid or brine (Sourirajan and Kennedy 1962; Bodnar et al. 1985). Thus, at the P and T of interest here, the equilibria are between three phases: aqueous vapor + brine + silicate melt. The vapor and brine coexist along a tie-line in P-T-x space and are isobarically and isothermally invariant (Fig. 1). Changes in the bulk chloride concentration are reflected by shifts in the mass proportion of vapor to brine.

The coexisting vapor and brine are not stable at room temperature and pressure. When an experimental run is quenched, the vapor and the brine remix to form the aqueous mixture (aqm). It is this quenched aqueous mixture that is analyzed. The design of the experiments does not permit elemental exchange between the aqueous vapor, the silicate melt, and the hydrosaline brine to be monitored directly. However, because changes in the ΣCl shift the

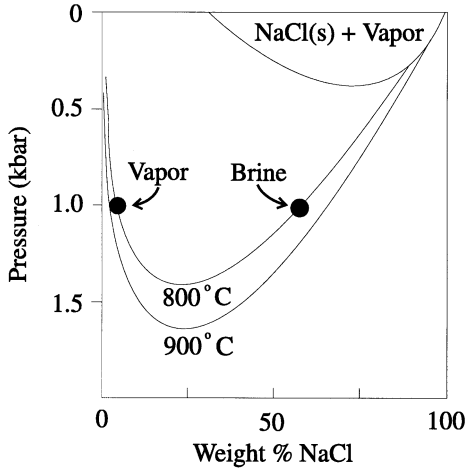

Fig. 1 Pressure- X_{NaCl} diagram of the system NaCl-H_2O with 800°C and 900° C isotherms (after Bodnar et al. 1985). *Solid circles* represent the approximate wt% NaCl concentration of the coexisting aqueous vapor (aqv) and hydrosaline brine (aqb) at 1 kbar and 800° C. Within the two-phase field, at a given pressure and temperature, the chlorine concentration (represented here as wt% NaCl) of the vapor and brine are fixed. Changes in the chlorine concentration of the quenched aqueous mixture (aqm) shift the mass proportion of vapor to brine along a tie-line between the two coexisting phases

vapor/brine ratio, plotting the $K_{j,k}^{aqm/mlt}$ vs ΣCl provides a relatively straightforward method for documenting the exchange equilibria for a given element pair, j and k, between the magmatic vapor and brine phases. For example, if the element-pair (j and k) have the same chemical affinity for the vapor and the brine, $K_{j,k}^{aqm/mlt}$ will not change systematically as the ΣCl increases or decreases (thus decreasing or increasing the vapor/brine ratio).

Silicate glass run products

The quenched silicate glass was recovered from the capsule as one or more rounded beads or small shards. Visual inspection of the glass revealed that they were generally colorless with zones of apparently clear glass juxtaposed with zones of milky white glass that were nearly opaque in some samples. Microscopic examination revealed three distinct types of fluid inclusions. The milky zones within the glass were due to a high density of small (< 1 mμ) diameter fluid inclusions that were labeled as type I. Microscopic examination of the glass also revealed two populations of larger (commonly > 10 mμ) fluid inclusions distributed throughout the glass fragments. Those consisting of mostly trapped vapor and small amounts of liquid were termed type II, and inclusions consisting of small vapor bubbles, liquid, and daughter crystals were termed type III. The fluid inclusion classification used above is based on the system employed by Nash (1976), and resembles the three populations of inclusions described by Shinohara et al. (1989).

Experimental results

Experimental results, presented in Table 2, are used to formulate Nernst-type partition coefficients, $D_{cu}^{aqm/mlt}$ and apparent equilibrium constants, $K_{Cu,Na}^{aqm/mlt}$. Fig. 2 shows the partition coefficient, $D_{Cu}^{aqm/mlt}$, as a function of total chlorine and HCl/ΣCl of the bulk aqueous mixture at 1 kbar, 800°C and 0.5 kbar, 850° C. The data in Fig. 2 demonstrate that the copper partitioning is non-Nernstian, and is a function of the total aqueous chlorine concentration. In addition, Fig. 2 shows that copper partitioning is pressure dependent with $D_{Cu}^{aqm/mlt}$ decreasing from 1 kbar (800° C) to 0.5 kbar (850° C).

Candela and Holland (1984) and Keppler and Wyllie (1991) demonstrated that the $D_{Cu}^{aq/mlt}$ (single aqueous phase + silicate melt) at 1.4 kbar (750° C) and 2 kbar (750° C) respectively, could be described as a linear function of the aqueous chlorine. In an attempt to fit linear regression lines to the partition coefficients (at 0.5 and 1 kbar) as a function of aqueous chlorine, we found that some data points plotted more than 1-sigma standard deviation away from the best fit line (Fig. 2). We conclude that the behavior of $D_{Cu}^{aqm/mlt}$ versus total chlorine is not a simple linear function. Candela and Holland (1984) used their experimental results to conclude that copper occurs in a monovalent (+ 1) state at magmatic temperatures and pressures. We have no evidence that would suggest that copper in these experiments occurs in a valence state other than + 1 also.

The most plausible explanation for the non-linear behavior of $D_{Cu}^{aqm/mlt}$ versus aqueous chlorine is vapor plus brine immiscibility. At magmatic temperatures and pressures, copper partitioning is between three phases, a low-salinity aqueous vapor, a hydrosaline brine, and the silicate melt. A $D_{Cu}^{aqm/mlt}$ (between the quenched aqueous mixture and the silicate melt) would be affected by vapor/melt partitioning at low total chlorine and by brine/melt partitioning at higher total chlorine concentrations. If the copper concentrations in the vapor and brine are different, which is a reasonable inference given the differences in their respective chlorine concentrations (Fig. 1), the aqueous mixture/melt partition coefficients would reflect differences in the mass proportion of low-salinity vapor to brine

In an attempt to place the experimental results in a more thermodynamically valid framework, we have formulated an apparent equilibrium constant expression for the exchange of copper and sodium between the silicate melt and the two-phase aqueous mixture. The pertinent exchange equilibria for copper and sodium between the low-salinity aqueous vapor (aqv), hydrosaline brine (aqb), and the melt are represented by the following simplified equations:

$$\mu_{Cuo_{0.5}}^{mlt} + \mu_{NaCl}^{aqv} = \mu_{CuCl}^{aqv} + \mu_{Nao_{0.5'}}^{mlt}, \quad (1)$$

and

$$\mu_{Cuo_{0.5}}^{mlt} + \mu_{NaCl}^{aqb} = \mu_{CuCl}^{aqb} + \mu_{Nao_{0.5'}}^{mlt}, \quad (2)$$

This thermodynamic formulation suggests that the raw Nernst (aqueous phase/melt) partition coefficient (D) for chloride-complexed elements is of limited utility. The scatter apparent in Fig. 2 does not propagate fully

Table 2 Copper partition coefficients ($D_{Cu}^{aqm/mlt}$) and average values for the apparent equilibrium constant ($K_{Cu,Na}^{agm/mlt}$) for copper-sodium exchange between the aqueous mixture (aqm) and the silicate melt (mlt)

	800°C and 1 Kbar							
Sample	C_{Cu}^{mlt} [a]	C_{Cu}^{aqm}	C_{Na}^{mlt}	C_{Na}^{aqm}	$D_{Cu}^{aqm/mlt}(+1\sigma)$	ΣCl[b]	HCl/ΣCl[c]	ASI[d]
Bt 4	15	1550	22900	1120	103(+26)	0.7	0.30	1.14
Bt 10	50	8100	18700	17800	160(+73)	3.3	0.30	1.20
Bt 11	50	6300	20200	8800	126(+58)	2.4	0.30	1.20
Bt 12	20	60	21500	300	3.0(+1.1)	0.2	0.30	1.11
Bt 13	25	100	20900	400	4.0(+0.7)	0.1	0.30	1.08
Bt 14	40	1100	22200	2200	27(+7.3)	0.8	0.30	1.08
Bt 16	25	7900	16400	13800	316(+110)	3.7	0.15	1.18
Bt 17	60	3500	20100	7000	58(+25)	1.9	0.15	1.06
Bt 18	20	600	21300	2700	30(+4.0)	0.6	0.15	1.07
Bt 20	15	6500	22900	29100	433(+24)	2.3	0.15	1.10
Bt 21	10	200	21000	1600	20(+5.1)	0.1	0.15	1.18
Bt 33	20	3800	18600	43000	190(+100)	3.2	0.03	1.14
Bt 45	20	6900	21200	24600	345(+110)	2.9	0.03	1.14
Bt 46	20	400	26200	4800	20(+12)	1.1	0.03	1.04

$K_{Cu,Na}^{aqm/mlt}$ (avg)[e] = 215 (+73) (HCl/ΣCl: 0.03–0.30)

[a] Concentration of element j in phase i (as % ppm)
[b] Total aqueous chlorine (mols/k of solution)
[c] The ratio of the HCl concentration in the starting aqueous solutions to the total aqueous chlorine
[d] ASI is the Aluminum Saturation Index of the silicate melt (ASI = molar A1203/ $(Na_2O + K_2O + 2CaO)$
[e] The average of the apparent equilibrium constant for copper-sodium exchange between the rhyolite melt and the two-phase aqueous mixture. Error is the standard deviation of the combined K-values

Table 2 (continued)

	850° C and 0.5 kbar							
Sample	C_{Cu}^{mlt}	C_{Cu}^{aqm}	C_{Na}^{mlt}	C_{Na}^{aqm}	$D_{Cu}^{aqm/mlt}(+1\sigma)$	ΣCl	HCl/ΣCl	ASI
Bt 25	340	5500	20600	11800	16(+2.3)	3.0	0.30	1.13
Bt 26	450	2000	21200	7350	4.4(+2.0)	1.6	0.30	1.10
Bt 27	10	200	24700	2400	2.0(+2.0)	0.9	0.30	1.06
Bt 28	4.0	20	21400	780	5.0(+4.6)	0.1	0.30	1.17
Bt 38	470	1060	19000	25200	2.3(+1.1)	3.0	0.03	1.07
Bt 39	80	120	22400	21500	1.5(+0.56)	1.5	0.03	1.01
Bt 40	50	20	21200	3600	0.4(+0.40)	0.5	0.03	1.10
Bt 41	30	3	23700	300	0.1(+0.04)	0.1	0.03	1.08

$K_{Cu,Na}^{aqm/mlt}$ (avg) = 11 (+6) (HCl/ΣCl: 0.03–0.3)

into the apparent equilibrium constants. Thermodynamic equilibrium constant expressions can be formulated from the chemical potentials to describe the elemental exchange within the three-phase system. However, because the vapor and brine were not analyzed directly it is more practical to formulate an apparent equilibrium constant by using concentrations from the quenched aqueous mixture:

$$K_{Cu,Na}^{aqm/mlt} = \frac{C_{Cu}^{aqm} \cdot C_{Na}^{mlt}}{C_{Cu}^{mlt} \cdot C_{Na}^{aqm}} \quad (3)$$

The compositions of the aqueous vapor and the brine are fixed and do not vary with changes in the total chlorine (ΣCl) of the aqueous mixture for a given bulk composition of the system at a specified temperature and pressure. Changes in ΣCl shift the proportions of vapor to brine along the tie-line. If $K_{Cu,Na}^{aqb/aqv}$ (between vapor & brine) is not on the order of unity, then $K_{Cu,Na}^{aqm/mlt}$ will vary with ΣCl.

Holland (1972) found that exchange constants for potassium and sodium between the melt and a single aqueous phase (at approximately 770° C-800° C and 1.5-2.5 kbar) displayed no systematic variation with aqueous chlorine. In this study the $K_{Cu,Na}^{aqm/mlt}$ display no apparent systematic variation over the range of chloride concentrations studied (approximately 0.1 to 3.7 mols/kg). $K_{Cu,Na}^{aqm/mlt}$ indicates that copper-sodium exchange between the melt, low-salinity aqueous vapor, and the brine is apparently independent of the relative mass proportions of vapor to brine.

Effects of melt composition on $K_{Cu,Na}^{aqm/mlt}$ and $D_{Cu}^{aqm/mlt}$

We attempted to evaluate the effects of melt composition on copper partitioning by varying the starting HCl/ΣCl. Based on the results of Urabe (1985), increasing the proton concentration (HCl at magmatic

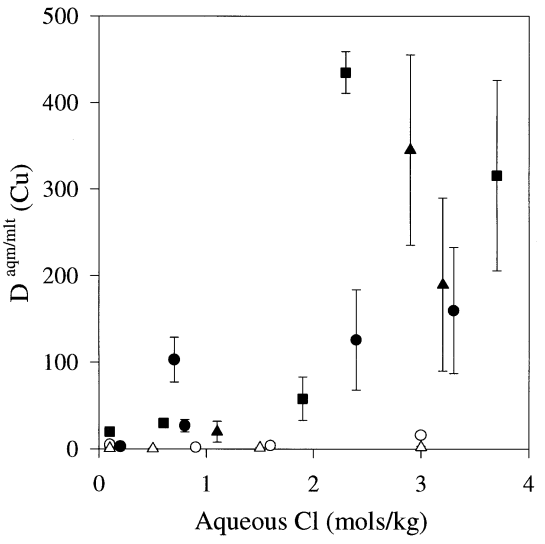

Fig. 2 The partition coefficient ($D_{Cu}^{aqm/mlt}$) for copper between a two-phase aqueous mixture and a high-silica rhyolite melt phase, at 1 kbar/800° C and 0.5 kbar/850° C, as a function of total aqueous chlorine and starting aqueous HCl/ΣCl. At 1 kbar: *solid circles* HCl/ΣCl = 0.30, *solid squares* HCl/ΣCl = 0.15, *solid triangles* HCl/ΣCl = 0.03. At 0.5 kbar: *open circles* HCl/ΣCl = 0.30, *open triangles* HCl/ΣCl = 0.03. Errors bars are 1-sigma standard deviation

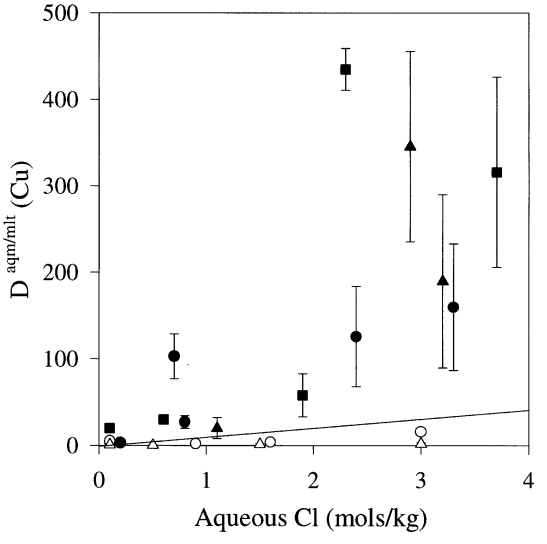

Fig. 3 The partition coefficient for copper, ($D_{Cu}^{aqm/mlt}$), from the silicate melt into a two-phase aqueous mixture, and a single phase aqueous fluid, as a function of total aqueous chlorine (ΣCl) at 1.4 kbar (750° C) (*solid line* from Candela and Holland 1984), 1.0 kbar (800° C), and 0.5 kbar (850° C) (symbols as in Fig. 2). Error bars are 1-sigma standard deviation

temperatures) should shift a metaluminous melt composition toward a peraluminous composition.

Results from this part of the investigation were inconclusive. Visual inspection of the data showed a possible, albeit tenuous, relationship between copper partition coefficients and the HCl/ΣCl in the starting solutions. However, no statistically significant correlation between the ASI of the silicate glass run products and $D_{Cu}^{aqm/mlt}$ or $K_{Cu,Na}^{aqm/mlt}$ could be demonstrated. We do not suggest that melt composition has no effect on copper partitioning, only that the results of this study do not demonstrate it beyond analytical uncertainty.

The effect of pressure on $K_{Cu,Na}^{aqm/mlt}$ and $D_{Cu}^{aqm/mlt}$

Fig. 3 and Table 3 contain the partition coefficients and apparent equilibrium constants from this study, and the $D_{Cu}^{aq/mlt}$ and $K_{Cu,Na}^{aq/mlt}$ (single aqueous phase/melt) from Candela and Holland (1984). Their starting materials were a synthetic granitic composition glass and a chloride-bearing aqueous solution that spanned a range of ΣCl similar to the present study.

Note that as pressure decreases, the equilibrium constants first increase, pass through a maximum, and then decrease sharply. Previous studies by Urabe (1987) and Webster et al. (1989) suggested that lower pressures favor the increased separation of the aqueous phase from the melt which in turn favors the segregation of metals such as Zn, Fe or REE into the aqueous phase.

Table 3 Apparent equilibrium constants, $K_{Cu,Na}^{aqm/mlt}$, for copper–sodium exchange between the aqueous mixture and the silicate melt. C and H (1984) is the $K_{Cu,Na}^{aq/mlt}$ from Candela and Holland (1984) for copper-sodium exchange between melt and a single aqueous phase

Reference	$K_{Cu,Na}^{aqm/mlt}$	Press./Temp.
This study	11(± 6)	0.5 kbar/850° C
This study	215(± 73)	1 kbar/800° C
C. and H. (1984)[a]	20(5.6)[b]	1.4 kbar/750° C

[a] Candela and Holland (1984)

[b] $K_{Cu,Na}^{aq/mlt}$ for copper–sodium exchange between melt and a single aqueous phase

The increase in copper-sodium exchange from 1.4 to 1 kbar (Table 3) agrees with this line of reasoning. However, at pressures less than 1 kbar, copper-sodium exchange decreases.

Modeling of copper-sodium exchange between silicate melt-aqueous vapor-hydrosaline brine

When an experimental charge is quenched to room temperature and pressure the immiscible aqueous vapor (aqv) and brine (aqb) remix to form the aqueous mixture (aqm). Direct determination of the concentration of a given element in the low salinity aqueous vapor or brine is not possible in the quenched solution. The aqueous mixture is analyzed as a bulk solution for the cations sodium and copper and for total chlorine.

From the concentrations in the aqm and the silicate melt, one can model the concentrations of a given element present in the coexisting aqueous vapor and brine at a specified temperature and pressure (Williams 1995).

The procedure for modeling the concentrations in the coexisting low-salinity aqueous vapor and the brine is detailed in Appendix 2. The method involves approximating the concentration of element i in the aqueous vapor by performing a single-phase experiment just outside the two-phase field along the low-salinity limb of the solvus. From this experiment an aqueous vapor "pin" is determined. The vapor "pin" is then used as an anchor to calculate a model concentration of element i in the brine by mass balance using the concentration of element i and total chlorine in the aqueous mixture.

Table 4 contains model brine/melt and brine/vapor partition coefficients, listed as $D^{*aqb/mlt}_{Cu}$ and $D^{*aqb/vap}_{Cu}$ respectively, and brine-melt ($K^{aqb/mlt}_{Cu,Na}$), and brine-vapor ($K^{aqb/aqv}_{Cu,Na}$) apparent equilibrium constant expressions for copper-sodium exchange (between the low-salinity vapor and the brine). The modeled $D^{*aqb/vap}_{Cu}$ indicate that copper partitions strongly into the brine relative to the aqueous vapor. $D^{*aqb/vap}_{Cu}$ also increase with decreasing pressure (Table 4). This behavior is most likely the product of increasing chlorine concentrations in the brine at 0.5 kbar versus chlorine in the brine at 1 kbar (Fig. 1).

Table 2 and Fig. 3 show that, at the lowest solution chlorine concentrations, $K^{aqm/mlt}_{Cu,Na}$ (representing copper-sodium exchange between melt and the low-salinity aqueous vapor) decreases with decreasing pressure. In addition, $K^{aqb/mlt}_{Cu,Na}$, which represents copper-sodium exchange between the silicate melt and the hydrosaline brine, also decreases with decreasing pressure (Table 4). This behavior indicates that the negative pressure dependence observed in $K^{aqm/mlt}_{Cu,Na}$ (between the quenched aqueous mixture and the silicate melt) occurs at magmatic temperatures and pressures between the three magmatic phase (vapor + brine + silicate melt).

Table 4 Modeled data for copper–sodium exchange between the coexisting aqueous vapor, hydrosaline brine, and the silicate melt

Press./Temp.	$D^{*aqb/mlt}_{Cu}$ [a]	$D^{*aqb/aqv}_{Cu}$	$K^{aqb/mlt}_{Cu,Na}$ [b]	$K^{aqb/aqv}_{Cu,Na}$
1 kbar/800° C	700	120	290	1.2
0.5 kbar/850° C	40	200	30	0.2

[a] $D^{*aqb/mlt}_{Cu}$ and $D^{*aqb/aqv}_{Cu}$ are the model partition coefficients for copper from the melt into the hydrosaline brine, and from the aqueous vapor into the hydrosaline brine respectively. D* are calculated from modeled copper concentrations in the hydrosaline brine and aqueous vapor, and empirically determined copper concentrations in the silicate glass

[b] $K^{aqb/mlt}_{Cu,Na}$ and $K^{aqb/aqv}_{Cu,Na}$ are the model apparent equilibrium constants for copper-sodium exchange between the melt, hydrosaline brine, and the aqueous vapor calculated using modeled and empirical copper concentrations as described above

A 1 kbar (800° C), despite a strong affinity for the high-salinity brine, the $K^{aqb/aqv}_{Cu,Na}$ are close to unity indicating that copper and sodium partition between the vapor and the brine in a similar fashion. The modeling shows that, at 1 kbar, in the salt-H_2O-rhyolite melt system, the effective partitioning of copper between the vapor and brine is dependent on the complexing of chlorine by sodium (and by extrapolation KCl as well), and not just on the total chlorine in the vapor or the brine.

Mavrogenes et al. (1993) reported copper values in the aqueous vapor and brine from synthetic fluid inclusions trapped in quartz at 700° C and 700 bars. Considering that both their Cu^{br}/Cu^{vap} ratios and our $D^{*aqb/aqv}_{Cu}$ were calculated from approximate concentrations in the vapor and brine, the brine/vapor ratios from their study and ours are roughly similar within an order of magnitude.

Implications for the origin of porphyry-copper deposits

Related studies

The association of porphyry-type deposits with relatively oxidized felsic magmatic systems has been confirmed in field studies of ore deposits worldwide (Lowel and Guilbert 1970; Gustafson and Hunt 1975; Titley and Bean 1981) In addition, investigations of the fluids associated with porphyry-type magmatic ore systems have confirmed that an aqueous phase or phases, usually enriched in chlorine and other volatiles, played an important role in the formation of ore deposits (e.g. Roedder 1979; Bodnar and Beane 1980).

From his investigation of the Yerington Batholith (Nevada) and its associated porphyry copper deposits, Dilles (1987) concluded that an orthomagmatic model, in which an aqueous phase exsolved, was key to the formation of the ore deposit at Yerington. He observed that during the differentiation of the pluton, whole-rock copper decreased by a factor of six and that the decrease could not be accounted for by segregation of copper by mineral phases during crystallization of the magma alone. In addition, halogen and water content from hydrous minerals, the presence of high-salinity fluid inclusions, and copper-rich quartz veins supported the hypothesis of the exsolution of a two-phase vapor + brine) halogen-bearing magmatic aqueous fluid. Dilles concluded that up to 80% of the copper in the melt was scavenged by the aqueous phases.

Investigations of copper rich fluid inclusions in the magmas erupted at the Valley of Ten Thousand Smokes by Lowenstern (1993) point to the presence of a copper enriched fluid associated with the magmas at the time of eruption. From his fluid inclusion data Lowenstern calculated apparent partition coefficients ranging from 30 to 190 for the inclusion/silicate pairs.

Although the values were high relative to published partitioning data, Lowenstern concluded that they were within the range of the partition coefficients determined in this and other experimental studies.

Additional evidence of ore-metal bearing fluids was gathered by an XRF microprobe study on copper-enriched vapor inclusions in pantellerites from Pantelleria, Italy (Lowenstern et al. 1991). The calculated apparent partition coefficients from the inclusion/silicate pairs averaged greater than 200. These apparent partition coefficients calculated from a naturally occurring magmatic system are similar to the values obtained at 1 kbar (800°C) in the present study.

The implications of pressure

In an attempt to explain the dichotomy in the behavior of $K_{Cu,Na}^{aqm/mlt}$ with decreasing pressure, the data are considered in the context of a melt saturated with an aqueous phase under polybaric conditions. One hypothesis is that as pressure drops two phenomena occur. The solubility of water in the melt, and the density of the aqueous phase(s) decrease. Within this framework we suggest a two-stage process to explain the polybaric partitioning data.

The degree of polymerization in a silicate melt is defined by the ratio of non-bridging oxygens that connect non-tetrahedrally coordinated cations to tetrahedrally coordinated cations (abbreviated as NBO/T, Mysen and Virgo 1986a,b). According to Mysen (1991) an essential consequence of the dissolution of water (as OH) in a silicate melt is to depolymerize the melt structure, or increase the NBO/T ratio.

If this process is viewed in reverse, as the pressure decreases water is expelled from the melt as its solubility decreases. This will free up OH-complexed cations to form network-building tetrahedra thus lowering the NBO/T and increasing the melt polymerization. The hypothesis is that as the pressure drops from 1.4 kbar (Candela and Holland 1984) to 1 kbar (this study) the melt polymerization increases, and an ore-metal cation such as Cu^+ experiences an increase in its chemical potential in the melt, enhancing its partitioning into the aqueous phases.

In addition to increasing the polymerization of the silicate melt, a decrease in pressure also decreases the density of the coexisting low salinity aqueous vapor and the hydrosaline brine. As the density drops, the "carrying power" of the aqueous mixture decreases (i.e. $[\partial\mu_{CuCl}^{aq}/\partial\rho^{aq}] < 0$). Thus at low pressures copper partitioning from the melt into aqueous vapor and brine would be inhibited by the physical changes in the density of the aqueous phases.

Estimates of the change in the density of the low salinity aqueous vapor can be made by using the Modified Redlich-Kwong equation of state (Kerrick and Jacobs 1981) to calculate the density of H_2O vapor at a given temperature and pressure. The compositions of the immiscible aqueous vapor can be approximated by using experimental data on the system H_2O-NaCl (Bodnar et al. 1985; Sourirajan and Kennedy 1962). At 800° C and 1 kbar the vapor would contain approximately 4.0 wt% NaCl, and at 850° C and 0.5 kbar the composition would be approximately 2.0 wt% NaCl. The substitution of water for the low salinity aqueous vapor in calculating densities is a reasonable extrapolation based on NaCl–H_2O vapor density data from Bischoff (1991).

Densities were calculated for 1.4 kbar (750° C), 1 kbar (800° C), and 0.5 kbar (850° C). The density at 1.4 kbars is 0.35 (gm/cm^3). At 1 kbar the density drops to 0.25 (gm/cm^3), and at 0.5 kbar it drops further to 0.12 (gm/cm^3). Over a pressure difference of 900 bars the density of the aqueous vapor decreases by almost 300%. This drop in the vapor density may be responsible for reducing copper and sodium partitioning from the melt into the low-salinity aqueous vapor.

However, this hypothesis does not successfully explain the decrease in $K_{Cu,Na}^{aqb/mlt}$ with decreasing pressure. An equation of state representing the volumetric properties of the system NaCl–H_2O at elevated temperatures was formulated by Anderko and Pitzer (1993), which was used to calculate molar volumes for coexisting aqueous vapors and brines to approximately 2 kbar and 900° C. Their data show that as pressure decreases from 1.0 kbar (800° C) to 0.5 kbar (800° C), density decreases from approximately 1.4 gm/cm^3 to 1.3 gm/cm^3, a change of approximately 9% while the $K_{Cu,Na}^{aqb/mlt}$ drops by almost a factor of 10 (Table 4). The density decrease in the brine with decreasing pressure in apparently of an insufficient magnitude to explain the decrease $K_{Cu,Na}^{aqb/mlt}$.

Two additional hypotheses are suggested to explain the drop in $K_{Cu,Na}^{aqb/mlt}$ with pressure. First, the increased viscosity in the silicate melt, due to increased melt polymerization at lower water contents, may trap brine-rich fluid inclusions in the quenched glass run product (Lowenstern, personal communication). This process would artificially lower copper concentrations in the aqueous mixture and increase copper concentrations in the quenched glass. A second hypothesis is that at lower pressures (0.5 kbar in this study) chlorine is preferentially retained in the silicate melt relative to the aqueous phase thus increasing the Cl/H_2O in the melt at 0.5 kbar versus 1 kbar. Chlorine in the silicate melt would complex with the copper thus inhibiting its partitioning into the hydrosaline brine and lowering $K_{Cu,Na}^{aqb/mlt}$.

The first hypothesis is unlikely. Recall that the hydrosaline brine could contain as much as 10 mols/kg chlorine. Incomplete phase separation of the brine would show up as anomalously low ΣCl in the quenched aqueous mixture, which was not observed. In addition, if a large number of brine inclusions are physically retained in the quenched glass, the electron

probe beam would intersect these trapped brine inclusions and in turn show up as anomalously high chlorine concentrations in the glass analyses. In this study when the probe beam did intersect a suspected inclusion, that analysis was rejected and redone at a new point.

The second hypothesis is more acceptable. Previous studies by Kilinc and Burnham (1972), Webster and Holloway (1988), Malinin et al. (1989), Shinohara et al. (1989), and Webster (1992) have demonstrated a negative dependence of the chlorine partition coefficient, $D_{Cl}^{aq/mlt}$, on pressure. In addition, Metrich and Rutherford (1992) found a moderate decrease in chlorine concentrations in rhyolite composition melts with increasing pressure. In an aqueous phase saturated melt, as pressure decreases, two phenomena occur. Chlorine concentrations in the melt increase relative to concentrations in the aqueous phase, and the water content of the melt decreases. This would increase the availability of chlorine in the melt relative to the hydroxyl. It is possible that at 0.5 kbars, Cu–Cl complexes in the melt are higher relative to melts at 1 kbar.

Discussion

The distinctive pressure dependence of the apparent equilibrium constant, $K_{Cu,Na}^{aqm/mlt}$, and the partition coefficient, $D_{Cu}^{aqm/mlt}$, could have an important bearing on the discussion of the depth of formation of porphyry copper deposits. When compared to copper-sodium exchange at 1.4 kbars (from Candela and Holland 1984), $K_{Cu,Na}^{aqm/mlt}$ first increases as the pressure decreases, passes through an apparent maximum at 1 kbar, and then decrease as pressure falls to 0.5 kbar. Experiments (Urabe 1987) involving Pb and Zn indicate that increasing pressure above 1.6 kbar suppresses ore metal partitioning up to at least 3.5 kbar. Interestingly, the data of Urabe (1987) also exhibit a maximum when the partition coefficient is plotted versus pressure. The data from Webster et al. (1989) indicate a lowering of partition coefficients to pressures of 4 kbar. The combined effect of suppressing copper partitioning above and below approximately 1 kbar could place limits on the depths for the most efficient removal of copper from the melt and its concentration in aqueous vapor and brine phases.

Aqueous phase saturation in a magma can be modeled by two idealized cases. Aqueous phase saturation can occur by the isobaric crystallization of anhydrous mineral phases (second boiling). Saturation by isothermal decompression of a hydrous magma or first boiling, is used to model the rise of a magma within the crust, and the model assumes that no crystallization accompanies aqueous phase saturation. In this model volatile exsolution is driven by the decreasing solubility of water in a silicate melt with decreasing pressure (Burnham 1979). The behavior of the copper-sodium apparent equilibrium constant with decreasing pressure observed in this study could have implications for the first boiling model.

If the probability of the formation of an ore deposit is discussed in terms of the chemical efficiency of removal, E(Cu) of copper (from the melt into the associated magmatic volatile phase, variables such as Cl/H_2O of the melt, depth, the $K_{Cu,Na}^{aqm/mlt}$, various crystal/melt partition coefficients (Lynton et al. 1993) melt composition, and the fugacities of volatiles (e.g. oxygen and sulfur) are critical. For example, if the Cl/H_2O of the melt is low, the chlorine concentration of the aqueous phase may be insufficient to scavenge copper from the melt. $C_w^{l,o}/C_w^{l,s}$, the ratio of the initial water content of a melt to the water content at aqueous phase saturation (Candela 1989a), is a critical variable controlling the timing of vapor saturation during second boiling (Candela 1989a). The results of the present study indicate that pressure exerts a control on the ability for copper to partition from the melt into the aqueous phase through variations in the $K_{Cu,Na}^{aqm/mlt}$. If aqueous phase saturation is delayed (at higher or lower pressures), copper may be sequestered by crystallizing mineral phases such as pyrrhotite (Lynton et al. 1993).

The physical efficiency of removal of ore-metals is just now coming under scrutiny. Candela (1991) asserted that depth of crystallization and the $C_w^{1,o}/C_w^{1,s}$ control the style of aqueous phase saturation. His model suggests that melts with high initial water content, or magmas that occurs at shallow depths in the crust, may form buoyant, bubble-laden plumes of ore-metal charged vapor, or spanning clusters of volatile phase conduits that provide a percolating network for aqueous fluids. If a melt has a low initial water content or intrudes too deep in the crust, any aqueous phase that exsolves may be trapped by the crystallizing magma (due to the low molar volume of the aqueous phase) and dispersed through a sub-solidus cracking front (Candela 1991). When the physical and chemical conditions for optimization of ore genesis are met within a given magmatic-hydrothermal environment, the probability of ore-formation is maximized.

Conclusion

At pressures and temperatures within the vapor-brine immiscibility field, the copper partition coefficient, $D_{Cu}^{aqm/mlt}$, increases with increasing chloride concentration in the aqueous mixture up to 3.7 mols/kg total chlorine, and is a function of total pressure. Variations in melt composition do not appear to affect copper partitioning.

Apparent equilibrium constants are formulated based on copper-sodium exchange equilibria between the silicate melt and the aqueous mixture. The lack of systematic variation of $K_{Cu,Na}^{aqm/mlt}$ with total chlorine

in the aqueous mixture indicates that, in the shift from a two-phase melt-aqueous vapor system to a three-phase melt-aqueous vapor-hydrosaline brine system, copper-sodium exchange is apparently independent of the mass proportions of vapor to brine. The average $K_{Cu,Na}^{aqm/mlt}$ at 1 kbar (800° C) was approximately 215. At 0.5 kbar (850° C) $K_{Cu,Na}^{aqm/mlt}$ was approximately 11.

When compared to copper-sodium exchange at 1.4 kbar (from Candela and Holland 1984), $K_{Cu,Na}^{aqm/mlt}$ first increases as the pressure decreases, passes through an apparent maximum at 1 kbar, and then decrease as pressure falls to 0.5 kbar. The concentrations of copper and sodium in the coexisting aqueous vapor and hydrosaline brine were modeled by using empirical data from the aqueous mixture, an aqueous vapor from two-phase experiments, and the high-silica rhyolite glass. Model brine/vapor partition coefficients, $D_{Cu}^{*aqm/mlt}$, indicate that copper partitions strongly into the hydrosaline brine relative to the low-salinity aqueous vapor. The model brine/vapor apparent equilibrium constant is close to unity. In addition, copper-sodium exchange between the brine and the silicate melt has a negative dependence on pressure.

The apparent maximum in the partitioning of copper relative to sodium is produced by a combination of a decreasing of water concentration in the melt with decreasing pressure, and either: (a) a decreasing density of the vapor phase with decreasing pressure or (b) the increasing of the chlorine concentration in the melt with decreasing pressure.

Appendix 1

List of abbreviations and symbols

aqm	chloride-bearing aqueous mixture (aqueous vapor + brine)
aqb	hydrosaline brine
aqv	low-salinity aqueous vapor
aq	single-phase (supercritical) aqueous vapor
C_i^j	concentration of element i in phase j
$D_{Cu}^{aqm/mlt}$	copper partition coefficient for the aqueous mixture and silicate melt
$D_{Cu}^{*j/k}$	model copper partition coefficient for the phase j and k (j/k = aqb/mlt and aqb/aqv)
$K_{Cu,Na}^{j/k}$	apparent equilibrium constant expression for copper-sodium exchange between the phases j and k
mlt	silicate melt (Bishop Tuff high-silica rhyolite glass)
ΣCl	total aqueous chlorine (Nacl + KCl + HCl + $CuCl_2$)

Appendix 2

Concentration in the low salinity aqueous vapor

If the bulk concentration of the element of interest in the aqueous mixture and an approximation of its concentration in one of the coexisting phases (vapor or brine) are known, the concentration in the other coexisting phase can be modeled by using the bulk aqueous total chlorine (ΣCl). Elemental concentrations in the immiscible aqueous vapor (aqv) are approximated by experiments conducted just outside the low salinity limb of the solvus in the NaCl-H_2O system. The concentration from this low salinity vapor is analyzed and used as a low salinity "pin" on the vapor-brine tie-line.

The first step in calculating an aqv concentration for a given element, i, is to determine a partition coefficient for that element from a single-phase (vapor-only) experiment. We assume that the following relationship holds:

$$D_i^{aq/mlt} = m(C_{Cl}^{aq}) \tag{A1}$$

(Holland 1972; Candela and Holland 1984) where $D_i^{aq/mlt}$ is the partition coefficient for element i between the aqueous phase and the silicate melt. m is the slope of the change in the partition coefficient with aqueous chlorine concentration (C_{Cl}^{aq}). $D_i^{aq/mlt}$ is defined as:

$$D_i^{aq/mlt} \equiv C_i^{aq}/C_i^{mlt}. \tag{A2}$$

C_i^{aq} is the concentration of element i in the aqueous phase and C_i^{mlt} is the concentration of i in the coexisting silicate melt. By rearranging Eq. A1 we can calculate a value for m:

$$m = D_i^{aq/mlt}/C_{Cl}^{aq}. \tag{A3}$$

Once we have a value for m it can be substituted in for the equation for the partition coefficient between the immiscible aqueous vapor (aqv):

$$D_i^{aqv/mlt} = m(C_{Cl}^{aqv}). \tag{A4}$$

C_{Cl}^{aqv} is the aqueous vapor (aqv) ΣCl which is fixed by compositions taken from the phase equilibrium experiments of Bodnar et al. (1985). By combining Eq. A4 with the generalized form of Eq. A2, we can solve for the concentration of element i in the aqv:

$$C_i^{aqv} = [m(C_{Cl}^{aqv})]\, C_i^{mlt}. \tag{A5}$$

Concentration in the hydrosaline brine

The concentration of the element of interest in the silicate melt, its concentration in the aqv, and the ΣCl of the aqm are combined to model the concentration of the element in the coexisting hydrosaline brine (aqb).

Changes in the bulk salinity of NaCl–H_2O system shift the proportions of the vapor to the brine but do not change the compositions of the vapor or the brine. Thus, the following general relationship can be formulated:

$$\text{Mass (aqv + aqb)} * C_i^{aqm} = \text{mass (aqv)} * C_i^{aqv} + \text{mass (aqb)} * C_i^{aqb} \tag{A6}$$

This equation can be rearranged and solved for C_i^{aqm}:

$$C_i^{aqm} = F^{aqv} * C_i^{aqv} + (1 - F^{aqv}) * C_i^{aqb} \tag{A7}$$

where:

$$F^{aqv} = \text{mass (aqv)/mass (aqv + aqb)}. \tag{A8}$$

F^{aqv} is a mass ratio variable that changes as the bulk composition of the aqm shifts along the vapor-brine tie-line. The next step is to relate F^{aqv} to changes in the bulk aqueous ΣCl and the chlorine concentrations in the coexisting aqv and aqb. Synthetic fluid inclusion data (from Bodnar et al. 1985) is used as an approximation for the chlorine concentration in the vapor and the brine:

$$C_{Cl}^{aqm} = [F^{aqv} * C_{Cl}^{aqv}] + [(1 - F^{aqv}) * C_{Cl}^{aqh}] \tag{A9}$$

where C_{Cl}^{aqv} and C_{Cl}^{aqb} are the vapor and brine chlorine values from Bodnar et al. (1985). Rearranging and solving Eq. A9 for F^{aqv} as a function of C_{Cl}^{aqm} produces:

$$F^{aqv} = (C_{Cl}^{aqm} - C_{Cl}^{aqb}/C_{Cl}^{aqv} - C_{Cl}^{aqb}). \quad \text{(A10)}$$

By reinserting Eq. A10 into Eq. A9 and rearranging variables the concentration of element i in the aqb (brine) can be modeled.

The relationship between the modeled aqv and the aqb is such that for a series of experiments performed along a single tie-line (at a fixed temperature and pressure), the composition of the aqv is fixed by the aqueous vapor "pin" derived by experiment. Variability in the system is revealed in compositional changes of the aqb, and is dependent upon the approximated composition in the aqv.

Acknowledgements Support for this project was provided by the National Science Foundation [EAR-9018870 (PAC) and EAR-9204671 (PAC)], and by the Department of Energy [DEF 6079ID13025 (PAC, PMP)]. We would like to acknowledge Drs. Jim Webster and Jake Lowenstern for providing thoughtful and constructive reviews of the manuscript. Thanks are due Gary Cygan of the United States Geological Survey for analytical and experimental assistance. Also, Marshall Reed, Steve Lynton, Kent Ratajeski, and the other members of the Laboratory for Mineral Deposits Research greatly assisted in the successful completion of this project.

References

Anderko A, Pitzer KS (1993) Equation-of-state representation of phase equilibria and volumetric properties of the system NaCl-H_2O above 573 K. Geochim Cosmochim Acta 57:1657–1680

Bischoff JL (1991) Densities of liquids and vapors in boiling NaCl-H_2O solutions: a PVTX summary from 300° C to 500° C. Am J Sci 291:309–338

Bodnar RJ, Beane RE (1980) Temporal and spatial variations in hydrothermal fluid characteristics during vein filling in preore cover overlying deeply buried porphyry copper type mineralization at Red Mountain, Arizona. Econ Geol 75:876–893

Bodnar RJ, Burnham CW, Sterner SM (1985) Synthetic fluid inclusions in natural quartz. III. Determination of phase equilibrium properties in the system H_2O-NaCl to 1000° C and 1500 bars. Geochim Cosmochim Acta 49:1861–1873

Brimhall, GH, Crerar DA (1987) Ore fluids: magmatic to supergene In: Carmichael ISE, Eugster HP (eds) Thermodynamic modeling of geological materials: minerals, fluids, and melts (Reviews in Mineralogy vol 16). Mineralogical Society of America, Washington DC, pp 235–321

Burnham CW (1967) Hydrothermal fluids at the magmatic stage: In: Barnes HL (ed) Geochemistry of hydrothermal ore deposits, 1st edn. Holt, Rinehart, and Winston, New York, pp 34–76

Burnham CW (1979) Magmas an hydrothermal fluids. In: Barnes HL (ed) Geochemistry of Hydrothermal Ore Deposits, 2nd edn. John Wiley and Sons, New York, pp 71–136

Burnham CW, Ohmoto H (1980) Late-state processes of felsic magmatism. Mining Geology Special Issue 8:1–11

Candela PA (1982) Copper and molybdenum in silicate melt-aqueous fluid systems. PhD dissertation, Harvard University

Candela PA (1989a) Magmatic ore-forming fluids: thermodynamic and mass transfer calculations of metal concentrations. In: Whitney JA, Naldrett AJ (eds) Ore deposits associated with magmas. Reviews in Economic Geology 4, El Paso, TX, pp 223–233

Candela PA (1991) Physics of aqueous phase evolution in plutonic environments. Am Mineral 76:1081–1091

Candela PA, Holland HD (1984) The partitioning of copper and molybdenum between silicate melts and aqueous fluids. Geochim Cosmochim Acta 48:373–380

Charles RW, Vidale R (1982) Temperature calibration of a new rapid-quench vessel. Am Mineral 67:175–179

Chou I-M (1978) Calibration of oxygen buffers at elevated pressures and temperatures using the hydrogen sensor. Am Mineral 63:690–703

Chou I-M (1987) Oxygen buffer and hydrogen sensor techniques at elevated pressure and temperature. In: Ulmer GC, Barnes HL (eds) Hydrothermal experimental techniques. John Wiley and Sons, New York, pp 61–99

Cline JS, Bodnar RJ (1991) Can economic porphyry copper mineralization be generated by a typical calc-alkaline melt? J Geophys Res 96(B5):8113–8126

Dilles JH (1987) Petrology of the Yerington batholith, Nevada: evidence for evolution of a porphyry copper ore fluids. Econ Geol 82:1750–1789

Gustafson LB, Hunt JP (1975) The porphyry copper deposit at El Salvador, Chile. Econ Geol 70:857–912

Hedenquist JW, Lowenstern JB (1994) The role of magmas in the formation of hydrothermal ore deposits. Nature 370:519–527

Hildreth, W (1979) The Bishop Tuff: evidence for the origin of compositional zonation in silicic magma chambers. Geol Soc Am Spec Pap 180:43–75

Holland HD (1972) Granites, solutions, and base metal deposits. Econ Geol 67:281–301

Keppler H, Wyllie PJ (1991) Partitioning of Cu, Sn, Mo, W, U, and Th between melt and aqueous fluid in the systems haplogranite-H_2O-HCl and haplogranite-H_2O-HF. Contrib Mineral Petrol 109:139–150

Kerrick D, Jacobs G (1981) A modified Redlich-Kwong equation for H_2O, CO_2, and H_2O-CO_2 mixtures at elevated pressures and temperatures. Am J Sci 281:735–767

Kilinc A, Burnham CW (1972) Partitioning of chloride between a silicate melt and coexisting aqueous phase from 2 to 8 kilobars. Econ Geol 67:231–235

Lowell JD, Guilbert JM (1970) Lateral and vertical alteration-mineralization zoning in porphyry ore deposits. Econ Geol 65:373–408

Lowenstern JB (1993) Evidence for a copper-bearing fluid in magma erupted at the Valley of Ten Thousand Smokes, Alaska. Contrib Mineral Petrol 114:409–421

Lowenstern JB, Mahood GA, Rivers ML, Sutton SR (1991) Evidence for extreme partitioning of copper into a magmatic vapor phase. Science 252:1405–1409

Lynton SJ, Candela PA, Piccoli PM (1993) An experimental study of the partitioning of copper between pyrrhotite and a high-silica rhyolite melt. Econ Geol 88:901–915

Malinin SD, Kravchuck IF, Delbove F (1989) Chloride distribution between phases in hydrated and dry chloride-aluminosilicate melt systems as a function of phase composition. Geochem Int 26:32–38

Mavrogenes JA, Bodnar RJ, Anderson AJ, Rivers M, Sutton S (1993) Metal distributions in immiscible fluids: evidence from synchrotron XRF analyses of synthetic fluid inclusions. EOS Trans Am Geophys Union 74:669

Metrich N, Rutherford MJ (1992) Experimental study of chlorine in hydrous silicate melts. Geochim Cosmochim Acta 56:607–616

Mysen BO (1991) Volatiles in magmatic liquids. In: Perchuk LL (ed) Progress in metamorphic and igneous petrology Cambridge University Press, Cambridge

Mysen BO, Virgo D (1986a) Volatiles in silicate melts at high pressures and temperatures. Part 1. Interaction between OH groups and Si^{4+}, Al^{3+}, Ca^{2+}, and H^+. Chem Geol 57:301–331

Mysen BO, Virgo D (1986b) Volatiles in silicate melts at high pressures and temperatures. Part 2. Water in melts along the join $NaAlO_2$-SiO_2 and a comparison of solution mechanisms of water and fluorine. Chem Geol 57:333–358

Nash JT (1976) Fluid inclusion petrology-data from porphyry copper deposits and applications to exploration. US Geol Surv Prof Pap 907-D:D1–D16

Nielsen W, Sigurdsson H (1981) Quantitative methods for electron microprobe analysis of sodium in natural and synthetic glasses. Am Mineral 66: 547–552

Roedder E (1971) Fluid inclusion studies of the porphyry-type ore deposits at Bingham, Utah, Butte, Montana, and Climax, Colorado. Econ Geol 66: 98–120

Roedder E (1979) Fluid inclusions as samples of ore fluids. In: Barnes HL (ed) Geochemistry of hydrothermal ore deposits, 2nd edn. John Wiley and Sons, New York, pp 684–737

Roedder E (1984) Fluid inclusions (Reviews in Mineralogy vol. 12). Mineralogical Society of America, Washington D.C.

Ryabchikov ID, Orlova GP, Efimov AS, Kalenchuk GE (1981) Copper in the system granite-fluid (in Russian) Geokhimia 9: 1320–1326

Shinohara H (1987) Partitioning of chlorine compounds in the system silicate melt and hydrothermal solutions. PhD dissertation Tokyo Inst. of Technology

Shinohara H, Iiyama JT, Matsuo S (1989) Partition of chlorine compounds between silicate melts and hydrothermal solutions: I. Partition of NaCl-KCl. Geochim Cosmochim Acta 53: 2617–2630

Sourirajan S, Kennedy GC (1962) The system H_2O-NaCl at elevated temperatures and pressures. Am J Sci 260: 115–141

Titley SR, Bean RE (1981) Porphyry copper deposits. Part 1. Geologic settings, petrology, and tectogenesis. Econ Geol, 75th Ann. Vol.: 214–235

Urabe T (1985) Aluminous granite as a source of hydrothermal ore deposits: an experimental study. Econ Geol 80: 148–157

Urabe T (1987) The effect of pressure on the partitioning ratios of lead and zinc between vapor and rhyolite melts. Econ Geol 82: 1049–1052

Webster JD (1992) Fluid-melt interaction involving Cl-rich granites: experimental study from 2 to 8 kbar. Geochim Cosmochim Acta 56: 659–678

Webster JD, Holloway JR (1988) Experimental constraints on the partitioning of Cl between topaz rhyolite melt and H_2O and $H_2O + CO_2$ fluids: new implications for granitic differentiation and ore deposition. Geochim Cosmochim Acta 52: 2091–2105

Webster JD, Holloway JR, Hervig RL (1989) Partitioning of lithophile trace elements between H_2O and H_2O-CO_2 fluids and topaz rhyolite melt. Econ Geol 84: 116–134

Whitney JA (1975) Vapor generation in a quartz monzonite magma a synthetic model with applications to porphyry copper deposits. Econ Geol 70: 346–359

Williams TJ (1995) Copper and HCl in felsic magmatic systems. PhD dissertation, University of Maryland